CSMA 2026
17ème Colloque National en Calcul des Structures
18-22 mai 2026, Presqu'île de Giens (Var)

Chemo-mechanical modeling of cement-aggregate composite affected by Delayed Ettringite Formation

C. Pelissou[1], F. Perales [1], L. Braysh[1], A. Socié[2]

[1] *ASNR, CEN Cadarache, France, celine.pelissou@asnr.fr, frederic.perales@asnr.fr, lama.braysh@asnr.fr*
[2] *CEA, DES, IRESNE, DEC, SESC, F-13108 Saint-Paul-Lez-Durance, France, adrien.socie@cea.fr*

Résumé —The aim of this work is to predict the behavior of mature concrete affected by Delayed Ettringite Formation (DEF) at the aggregate scale. A sample composed of CEM I cement paste bonded to siliceous aggregate have been simulated with the chemo-poromechanical XPER code. The initial degradation at the paste/aggregate interface was studied, and the results show that the initial state influences ettringite precipitation and therefore cracking. Good agreement with crack propagation and swelling evolution is obtained in comparison with experimental data, but kinetics need to be improved.
Mots clefs — Delayed Ettringite Formation, Multiphysics modeling, Frictional Cohesive Zone Model.

1. Introduction

During the lifetime of concrete structures, delayed deformation and chemical reactions can degrade the material and diffusion properties of the concrete materials. Some sources of these delayed stresses might also be internal. For instance, when hydrated concrete experiences is subjected to high curing temperatures during its early stages, sodium leaching can cause a reaction between the sulfates present in the concrete mix and calcium aluminate, producing ettringite, which forms and precipitates inside the pores of the concrete. This causes swelling and microcracks and macrocracks, which eventually propagate, increasing the swelling and leading to a loss of mechanical strength and, ultimately, deterioration of the concrete structure. This pathology is known as Delayed Ettringite Formation. The phenomena and parameters governing DEF are multiscale and Multiphysics, with the microstructural properties of concrete affecting swelling behavior [7]. It is thus important to study the mesoscale pathology as well as the effect of cracks on concrete affected by DEF.

In this work [8], we are interested in characterizing and monitoring the chemical and mechanical behavior of mature concrete affected by Delayed Ettringite Formation. In order to better understand the local phenomena, 3D numerical simulations of cement-aggregate samples are performed to study the ettringite formation at the mesoscale, using a coupled transport-chemo-poromechanical model [3] developed in the XPER code [2]. The results are compared with previous experimental work [1].

2. Experimental case study

A previous experimental work has been done to study the DEF pathology at the mesoscale and to identify the location of degradation at the cement paste/aggregate interface [1]. Illustrated on Figure 1 (left), the sample was a composite prismatic sample composed of siliceous aggregates bonded by a Portland cement paste (CEM I 52.5 R) of dimensions 10×10×30 mm^3 with a Water/Cement ratio of 0.47. The chemical composition of cement paste is presented in Table 1. The choice of materials and the addition of Na_2SO_4 promoted the formation of DEF [1].

Table 1 – Chemical composition of CEM I 52.5 R [1]

Components	K_2O	SO_3	Fe_2O_3	Al_2O_3	MgO	Na_2O	Na_2O_{eq}
Content (%)	0.35	3.59	3	4.15	1	0.16	1.2

The samples underwent a hydrothermal treatment in a climate chamber while maintaining a relative humidity of 95%, by an increase in the temperature by 5°C/hour, from 20°C, before being preserved at 80°C for 2 hours. This step has been done directly after their manufacture. After applying this thermal cycle, the samples were preserved in a distilled water tank (that have not been changed) at a temperature of 38°C. The expansion of the samples was tracked using the image correlation technique by a speckle pattern placed on one side of the sample and later following the development of the pathology by taking images of this face each seven days. The expansion curve is plotted in Figure 1 (right). Furthermore, the local mineralogy was studied using scanning electron microscopy, which revealed the presence of ettringite at the interface. The authors analyzed that the formation of ettringite had no impact on local swelling, as ettringite precipitated locally in the form of parallel needles, but it could have an influence on the tensile strength of the interface [1].

The chemo-poromechanical model, developed in [3], [4] and presented in the next section, is validated thanks experimental data from this study (initialization of parameters based on the chemical composition of the cement paste).

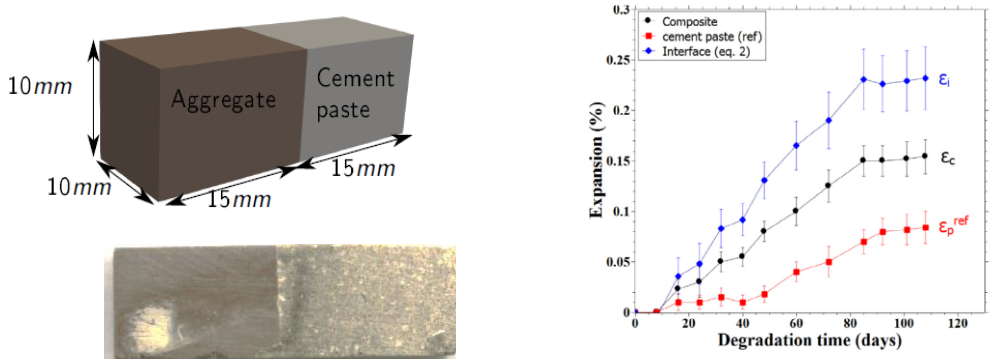

Figure 1 – Left, composite sample (scheme and real specimen). Right, average expansions of the experimental composite stored in distilled water tank at 38°C versus degradation time [1].

3. Chemo-poromechanical model

The chemo-poromechanical model couples a reactive transport model with a poromechanical model. This model aims to predict the swelling caused by chemical species precipitation and its mechanical consequences, in particular the initiation and propagation of cracks. Fracture analysis is performed using a micromechanical model based on a multibody concept and the Frictional Cohesive Zone Model (FCZM) [2], [3].

3.1. Reactive transport model

The reactive transport model describes the evolution of mineralogy in fractured concrete. For each time step, species transport and geochemical equilibrium are solved sequentially. In this model, the geomaterial is assumed to be fully saturated, and the transport of ions to be driven by the concentration gradient of the species. Ion transport follows Fick's law formulated in terms of concentration:

$$\frac{\partial \emptyset C_i^{aq}}{\partial t} = \nabla.\left(D_i \nabla C_i^{aq}\right) + \frac{\partial \emptyset (C_i^{aq})^{\Xi}}{\partial t} \quad \textbf{(1)}$$

Where C_i^{aq} [mol.L^{-1}], D_i [m^2.s^{-1}] and $\emptyset$ represent the concentration, the effective diffusion coefficient of species, and the porosity respectively. The last term acts as a source/sink term, accounting for the creation or consumption of ion in solution due to chemical reactions [mol.L^{-1}.s^{-1}].

In the chemical solver, chemical processes are assumed to be in thermodynamic equilibrium. Electroneutrality is imposed and chemical reactions are assumed to be reversible and instantaneous.

We consider solid, aqueous and sorption reactions. The chemical model of the DEF takes into account the link between sulfate sorption and sodium leaching. The solid reactions are described in Table 2 whereas the sorption reactions in Table 3.

Table 2 – Solid reactions used for DEF simulations [4]

Chemical equations	$\log_{10}(K)$
Portlandite $\Leftrightarrow Ca^{2+} + 2OH^-$	-5.19
Katoite $\Leftrightarrow 2Al(OH)_4^- + 3Ca^{2+} + 4OH^-$	-20.5
Ettringite $\Leftrightarrow 2Al(OH)_4^- + 6Ca^{2+} + 3SO_4^{2-} + 4OH^- + 26H_2O$	-44.9

Table 3 – Sorption reactions used for DEF simulations [4]

Chemical equations	$\log_{10}(K)$
$\equiv Si{-}OH + Ca^{2+} + OH^- + SO_4^{2-} \Leftrightarrow \equiv Si{-}OCaSO_4^- + H_2O$	7.3
$\equiv Si{-}OH + Na^+ + OH^- + SO_4^{2-} \Leftrightarrow \equiv Si{-}ONaSO_4^{2-} + H_2O$	5.8

3.2. Poromechanical model

The poromechanical model is composed of two parts: one which handles the volumetric behavior, i.e. the poromechanics of safe material, and another which handles the surface behavior responsible for the cracks. The volumetric behavior part aims to estimate the mechanical and diffusive parameters and to identify the expansion caused by significant solid precipitation in a porous medium described by an isotropic elastic poromechanical model [3]. This resolution is based on the Biot formulation where the pressure is influenced by the volume fraction of the primary precipitated solid and the strain tensor [3], [4]:

$$\sigma = \mathbb{C}: \varepsilon - bPI$$

$$P = N \langle \varphi_s - \langle \varphi_s^0 + b \, tr \, \varepsilon \rangle + \rangle + \quad \textbf{(2)}$$

where σ is the Cauchy stress tensor [Pa], $\mathbb{C}$ is the fourth-order stiffness tensor [Pa], ε is the linearized strain tensor, P is the pore pressure [Pa], I is the identity second-order tensor, b is the Biot coefficient assuming overall isotropy [−], N is the Biot skeleton modulus [Pa], and $\langle x \rangle = (x + |x|) / 2$ are the Macaulay brackets. φ_s is the main precipitated solid (here, the ettringite) and $\varphi_s^0 \in [0,1]$ is a model parameter that represents the quantity of initial pores to be filled with solid precipitates to induce swelling. We use the subscript *s* to define the variable associated with the main solid phases. The pore pressure will eventually cause stress and local swelling.

For the initiation and propagation of cracks and post-fracture phenomena, we use the so-called Frictional Cohesive Zone Model (FCZM) which relates the cohesive stress R_{adh} [$Pa.m^{-1}$] to the displacement jump of the crack lips [u] [m] by a damageable surface second order stiffness tensor $K(\beta)$ and considers the post fracture pressure such that:

$$R_{adh} = K(\beta) \cdot [u] \quad \textbf{(3)}$$

The parameter β represents the adhesion of the interface: value of 1 corresponds to a sound interface and β=0 demonstrates a totally broken interface. The cracks that are initiated and propagated in the material alter the diffusion of the chemical solution [4].

3.3. Chemo-poromechanical coupling

The coupling strategy follows a sequential iterative approach. At each time step, reactive transport is calculated through a fixed point (species transport and geochemistry), followed by the poromechanics of the solid phases. A small time step is mandatory for the computation of the Frictional Cohesive Zone Model and the diffusive time step is scaled [4]. These physical models have been implemented in XPER code (eXtented cohesive zone models and PERiodic homogenization) [2], used in this study.

Since the cement paste is considered mature here, the first step in the simulations requires, on the one hand, estimating the initial chemical parameters by calculating hydration to estimate the microstructure and initial concentrations and, on the other hand, estimating the mechanical parameters by analytical homogenization to evaluate the diffusive and poroelastic parameters [5]. In this work, the value of φ_s^0 is assumed to be 10^{-3} [4].

4. Numerical application

4.1. Data setup

The numerical application deals with a composite sample ($1\times1\times3$ cm^3) composed of a cement paste matrix connected to an aggregate (see Figure 2 left) placed along its longest side (the bottom side is blocked). The matrix phase is composed of a CEM I cement paste based on the mix described in the experimental work of Jebli (see Table 1). The initial chemical properties (see Table 4) and the initial mechanical parameters (see Table 5 and Table 6) were estimated based on the experimental data. At the boundaries, concentration 10^{-7} mol.L^{-1} is imposed for hydroxide OH^- and sodium Na^+ and a null concentration for the aqueous species, since the sample was immersed in water during experiments. The mechanical time step dt is 5×10^{-8} s, the diffusion time step is 1 hour. The mesh size used is 1mm with 29236 tetrahedral meshes (see Figure 2 right).

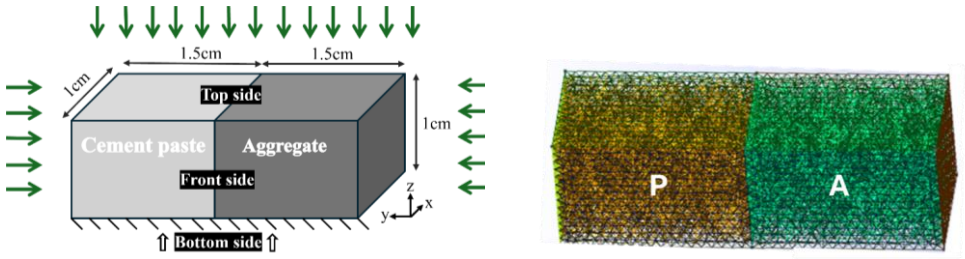

Figure 2 – Left, numerical sample composed of cement paste and aggregate. The top, front and bottom sides represent the predefined sides of the sample. Right, meshed sample (P paste and A aggregate).

4.2. Estimations of input parameters

The cement paste is considered mature. So, a initial step is required to estimate the initial chemical and mechanical parameters that will be used. A detailed explanation on the procedure is presented in following studies [3], [4], [5], [6].

Table 4 – Estimated initial chemical parameters

Chemical component	Ca^{2+}	OH^-	SO_4^{2-}	Al^{3+}	Na^+	$Si{-}ONaSO_4^{2-}$	$Si{-}OCaSO_4^-$
Concentration ($mol.L^{-1}$)	5.8×10^{-3}	6.5×10^{-2}	4.7×10^{-5}	1.6×10^{-5}	5.3×10^{-2}	0.1	0.2

Chemical component	Portlandite	Katoite	Ettringite	CSH
Concentration ($mol.L^{-1}$)	20.6	1.5	0.7	16.5

Table 5 – Initial mechanical parameters. The initial value of φ_s^0 is assumed.

D [$m^2.s^{-1}$]	**ν**	**E [GPa]**	**b**	**N [MPa]**	φ_s^0
2900	0.25	19.16	0.27	175×10^9	10^{-3}

Table 6 – Initial cohesive parameters.

σ_I **[Pa]**	σ_{II} **[Pa]**	ω_I **[$J.m^{-2}$]**	ω_{II} **[$J.m^{-2}$]**
4.6×10^7	46×10^7	20	200

4.3. Parametric study: effect of initial interface degradation on the DEF progression

For a composite sample, the interface between the cement paste and the aggregate can alter the chemical transport and hence the diffusion and precipitation of ettringite. This would eventually lead to a change in the cracks pattern. Here, we focus on the effect of interface adhesion through an initial crack on the DEF pathology. In the model, the initial crack at the interface between cement paste and aggregate is monitored by the initial value of β in equation (3). Different initial values are considered: from initially sound interface (β =1) without any crack towards a totally cracked interface (β =0) and so an initial gap between cement and aggregate.

In the simulations, cracks initiate due to the precipitation of ettringite inducing swelling, then propagate in the sample, causing at a later stage the deterioration of the interface. Gaps appear between the paste and aggregate which favors the precipitation of solids. Figure 3 show the ettringite precipitation (left image) and the resulting cracks that formed in the top side of the cement paste (left image), for an initial β value of 0.6. The cracks form close to the boundary as a result of the precipitated ettringite which is also affected by the boundary conditions. This concave shape of ettringite causes a higher stress parallel to the boundary and hence this shape of cracks is formed in the top side of the sample. The ettringite precipitation creates such cracks in the top side of the sample, however, a cracked interface would lead to a change in the pathology once these initial cracks widen and propagate through the sample. This is mainly because cracks alter diffusion, leading to precipitation.

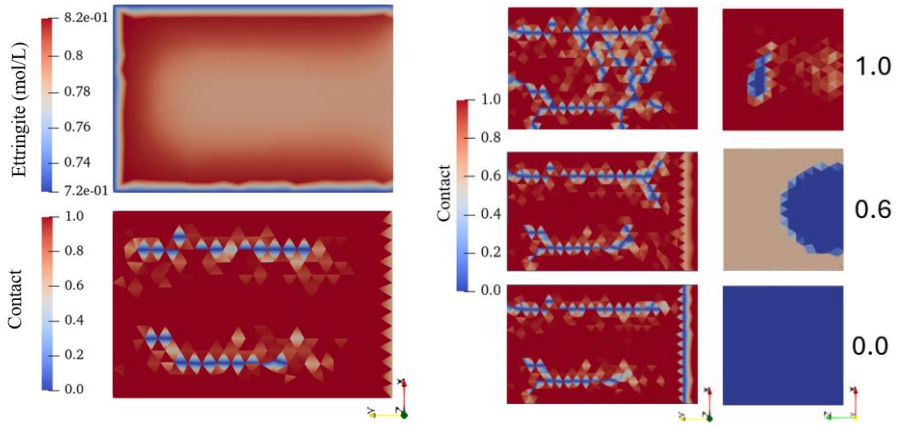

Figure 3 – Left, ettringite precipitation (top side of sample) and the resulting crack path for β=0.6 after 4.5 days. Right, effect of initial interface cracking on the crack propagation after 12 days. Colors represent β parameter (blue is 0 and red is 1).

To demonstrate the effect of the initial degradation of the interface, the DEF pathology is compared at 12 days for three samples with initial β values of 0, 0.6 and 1 (see Figure 3). For β = 0, the interface is totally cracked. For β = 0.6, the cracks initiate where part of the interface is totally broken (the blue colored part) and the rest is partially cracked. For β = 1, part of the interface remains totally sound while a small part begins to crack. As a result of this difference at the interface level, the cracks path in the top face varies between these samples. This is due to the difference in the stress caused by the precipitated ettringite and the different locations of the initial cracks.

Figure 4 presents a cross section in the yz plane in the middle of the sample for β = 0.6. We can see the ettringite precipitation near the boundaries and interface (the dark red color) along with the resulting cracks, which demonstrates the effect of the precipitated ettringite on the crack formation. The cracks formed in the zones have higher ettringite precipitation (values between 0.8 and 0.82). Initially ettringite precipitated at the boundaries induces crack by differential stress (swelling in the attack area). Then the sodium leaching is localized and accelerated inside the crack that induced ettringite near cracks. The sodium is essential for ettringite formation, meaning that cracked zones, where ettringite precipitation is more pronounced, have lower sodium availability (see the middle image of Figure 4). Additionally, katoite dissolution provides the necessary Al^{3+}, further promoting ettringite formation. This also explains why katoite concentrations are lower inside cracks (see the right image of Figure 4), where ettringite precipitation is favored. In conclusion, Figure 4 highlights the capacity of the model to predict complex chemo-mechanical phenomena.

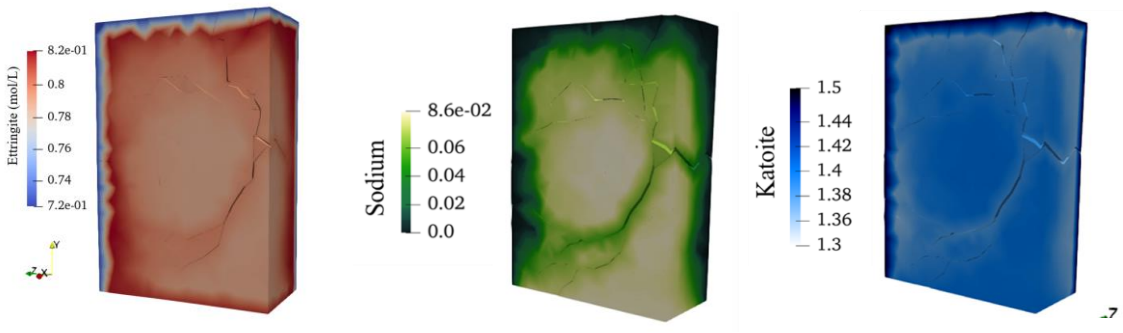

Figure 4 – Cross section of the sample with initial β=0.6 at the interface. The color bar represents the concentration of ettringite, sodium and katoite; the crack width is scaled by a value of 3.

4.4. Comparisons with experiments

The pathology performed in the simulation for β = 0.6 is compared to the pathology that was observed in experiments in Figure 5. The top/left image presents one sample taken from the experimental work [1] and the figure below shows the prediction of pathology obtained numerically. We can clearly notice the lines parallel to the boundary in experiment and a similar result is obtained in this simulation.

The expansion is measured using numerical sensors located in the cement paste and the aggregate as illustrated in Figure 5. The sensors used are of large band width, that is the size of the sample width. The value computed by each sensor is the average value of displacement of all the points located through the sensor which is equivalent to averaging values given by several sensors. To compute the expansion, we consider the difference between the values of displacement obtained by each sensor (the one placed on the cement paste and the one on the aggregate), and we divide by the initial distance separating them.

Figure 5 (right) shows the expansion ε_c (%) as a function of time (days) for the samples with different initial β values (between 0 and 1). In this plot, we can see that the expansion does not begin instantly for all values of β, and the value remains zero for some time before it starts increasing. For the sample with initial β = 0, the expansion is nearly increasing linearly with time, because of the cracks that are created in the cement paste region. The expansion for initial β = 0.6 reaches its maximum value (0.2%) at nearly 15 days. And the expansion of the sample with initial β = 1, increases at the beginning then increases slightly with time. Comparing these curves to ε_c obtained in experiments (see Figure 1), we notice that the shape provided for initial β = 0.6 is the closest to that of experiments. But this expansion value is higher, and the kinetics is too high, however this can be linked to effect of the interface or the simple hydration model. Due to this specific initial value of β, the cracks at the interface widen and expand until the interface totally breaks at nearly 10 days, causing greater expansion than in experiments, where the aggregate and cement paste were not totally separated. The shape obtained in the experiments differs from that of initial β = 1 and β = 0, confirming that, in the experiments, the interface between the cement paste and the aggregate has some gaps or cracks (hence initial β cannot be 1) and clearly is not totally cracked (β cannot be 0). The hypotheses assumed for cement paste composition makes it difficult to obtain same quantitative values obtained in experiments. However, in these simulations, we obtain the same expansion shape and evolution, and a good crack path compared to the experimental sample.

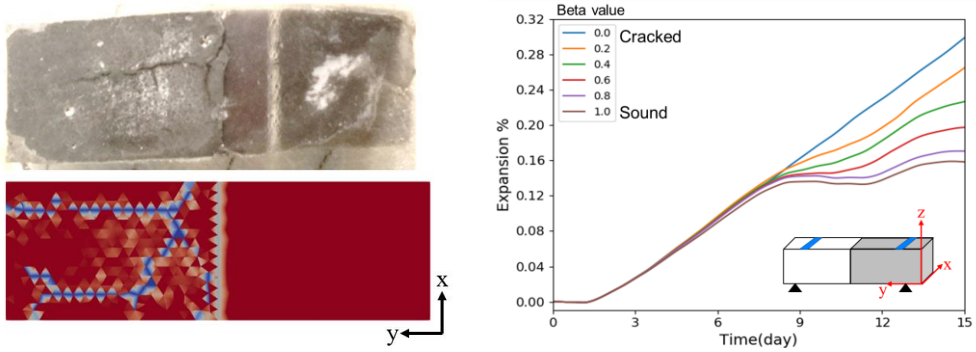

Figure 5 – Left, cracks pattern of top side sample: image of experimental composite (on top) and from simulation (at bottom) with initial β = 0.6. The cement is at left, the aggregate at right. Right, numerical expansions (%) for different initial β as a function of the time (day). The image at the bottom right illustrates the placement of the 2 sensors (indicated in blue) in the top side of numerical sample.

5. Conclusions

This study is based on numerical complex modeling of the behavior of a composite specimen degraded by internal sulfate reaction at the aggregate scale. The prediction of this pathology using the XPER chemo-poromechanical model gives good agreement. A parametric study on the effect of the interface degradation between cement paste and aggregate is performed. This study demonstrates the effect of initial damage on the progression of pathology in the sample and near the interface. Coherent tendency on chemical species diffusion inside cracks is obtained. The crack patterns and the expansion of the numerical sample are qualitatively in accordance with experimental data, but kinetics need to be improved.

6. Acknowledgments

The project ACES (Towards improved Assessment of safety performance for LTO of nuclear Civil Engineering Structures) has received funding from the Euratom research and training program 2019-2020, under grant agreement No.900012. The authors thank the EU and all the ACES contributors for their support and contributions.

Références

[1] M. Jebli, F. Jamin, C. Pelissou, E. Lhopital, and M. S. E. Youssoufi. Characterization of the expansion due to the delayed ettringite formation at the cement paste-aggregate interface, Construction and Building Materials, vol. 289, p. 122979, 2021.

[2] F. Perales, F. Dubois, Y. Monerie, B. Piar, and L. Stainier. A NonSmooth Contact Dynamics-based multi-domain solver: Code coupling (Xper) and application to fracture. European Journal of Computational Mechanics, vol. 19, p. 389-417, 2010.

[3] A. Socié, F. Dubois, Y. Monerie, and F. Perales. Multibody approach for reactive transport modeling in discontinuous-heterogeneous porous media, Computational Geosciences, vol. 25, no 5, p. 1473-1491, 2021.

[4] A. Socié, F. Dubois, Y. Monerie, M. Neji, and F. Perales. Simulation of internal and external sulfate attacks of concrete with a generic reactive transport-poromechanical model, European Journal of Environmental and Civil Engineering, vol. 27, no 12, p. 3679-3706, 2023.

[5] A. Socié, Y. Monerie, and F. Péralès. Effects of the microstructural uncertainties on the poroelastic and the diffusive properties of mortar, Journal of Theoretical, Computational and Applied Mechanics, p. 8849, 2022.

[6] J. Pouya, M. Neji, L. De Windt, F. Péralès, A. Socié, and J. Corvisier. Investigating chemical and cracking processes in cement paste exposed to a low external sulfate attack with emphasis on the contribution of gypsum, Construction and Building Materials, vol. 413, p. 134845, 2024.

[7] Al Shamaa, M., Lavaud, S., Divet, L., Colliat, J. B., Nahas, G., & Torrenti, J. M. (2016). Influence of limestone filler and of the size of the aggregates on DEF. Cement and Concrete Composites, 71, 175–180.

Braysh, L., Pelissou, C., Perales, F. & Socié, A. Coupled transport-chemo-mechanical simulation of cement/aggregate samples affected by DEF at the aggragate scale. Effects of pre-cracked interface and comparison with experimental data. FRAMCOS-12, L.A. Pichler, Ch. Hellmich, P. Preinstorfer (Eds), 2025.